ANALYSIS OF HIGH SPEED SQUIRREL CAGE INDUCTION MOTOR WITH INFLUENCE OF RIVETING

Jiří Klíma

Doctoral Degree Programme (1), FEEC BUT

E-mail: xklima14@stud.feec.vutbr.cz

Supervised by: Ondřej Vítek

E-mail: *viteko@feec.vutbr.cz*

Abstract: This paper deals with analyzing of high speed squirrel cage induction motor and the influence of riveting stator stack. The model of high speed induction motor was made in ANSYS Maxwell software in accordance with provided design documentation. Test bench was used to experimentally verify the results. The difference between measurement and simulation are explored. Distribution of the losses and its individual portion are discussed at the end. Stator sheets are riveted and influence of rivets will be subject of the interest.

Keywords: high-speed induction motor, test bench, finite element method, riveting

1. INTRODUCTION

It is well-known that the output power of the rotating machines is proportional to rotating speed. Frequency converter are used to provide variable speed by variable input frequency. The ratio between size of the machines and the output power can be changed by angular speed. High speed induction machines (IM) has been investigated due to small size and good dynamic performance [1]. The high speed IM are nowadays used as drives in compressor, vacuum pump, spindles, turbine generator [1] [2] [3] and in some cases even in automotive industry.

Two concept of high speed IM are used. The first includes using of solid rotor. Solid rotor can resist mechanical stress and according to [2], the circumferential speed can reach up to 460 m/s. However, the electromagnetic properties tends to be very poor even with features modification (axially slitted rotor, copper coated rotor). The second option is classical lamination rotor with squirrel cage. High speed IM with appropriate squirrel cage can reach circumferential speed up to 200 m/s, see in [2]. Our test motor with squirrel cage has a circumferential speed of 40 m/s.

Due to high input frequency from laboratory supply, the analysis of power loss made by hysteresis and eddy current become very important. Hysteresis loss are caused by alternating magnetization of stator sheets. Hysteresis curve for supply frequency is required for correct computation of the losses. Due to a great variety of supply frequency, it is almost impossible to find a single expression for total loss of stator sheet. In practice, we are satisfied with data from the manufacturer, although this data can be inaccurate by manufacturing process or for frequency domain incomplete, see [7].

Data provided from manufacturer is not fully take into account the manufacturing process. The cutting and punching of steel sheets have significant influence on sheets material properties. It was shown in [4] [6] that cutting and punching introduce material stress and thus the electric losses in the sheets will increase. Furthermore, the stacking process has significant role too. There are several methods how to assemble lamination sheets into a stator core. Welding process destroys insulation between lamination sheets and cause short circuit and lead to extra eddy current losses. The welds have to be keep out main flux path to minimize shorting. Riveting process is more economical and reliable method how to assembly stator core but it requires punching small holes [5].

2. FINITE ELEMENT MODEL OF HIGH SPEED MOTOR

Model has been simulated in ANSYS Maxwell software package. Geometry, material, mesh and boundary condition was created in pre-processor. The sheet for stator and rotor with indication M700-50A was used in simulation. The BH curve of the sheet was defined from B = 0.2 T to B = 1.5 T. This range was not satisfactory, therefore the BH curve was extrapolated up to B = 1.9 T. Steel with indication *1008* and conductivity of σ = 22 MS/m was used for shaft.

Mesh and sampling time are very important aspects. Mesh and sampling time have to be in balance between computing time and accuracy. Motor is supply by frequency of f = 330 Hz. Our sampling time, to provide sufficient results, was set to be T_s = 30 μs. The sampling time was set intentionally to make more than N = 100 samples during one period. The number of samples is deemed as sufficient. The whole finite element model of motor is shown in Fig.1.

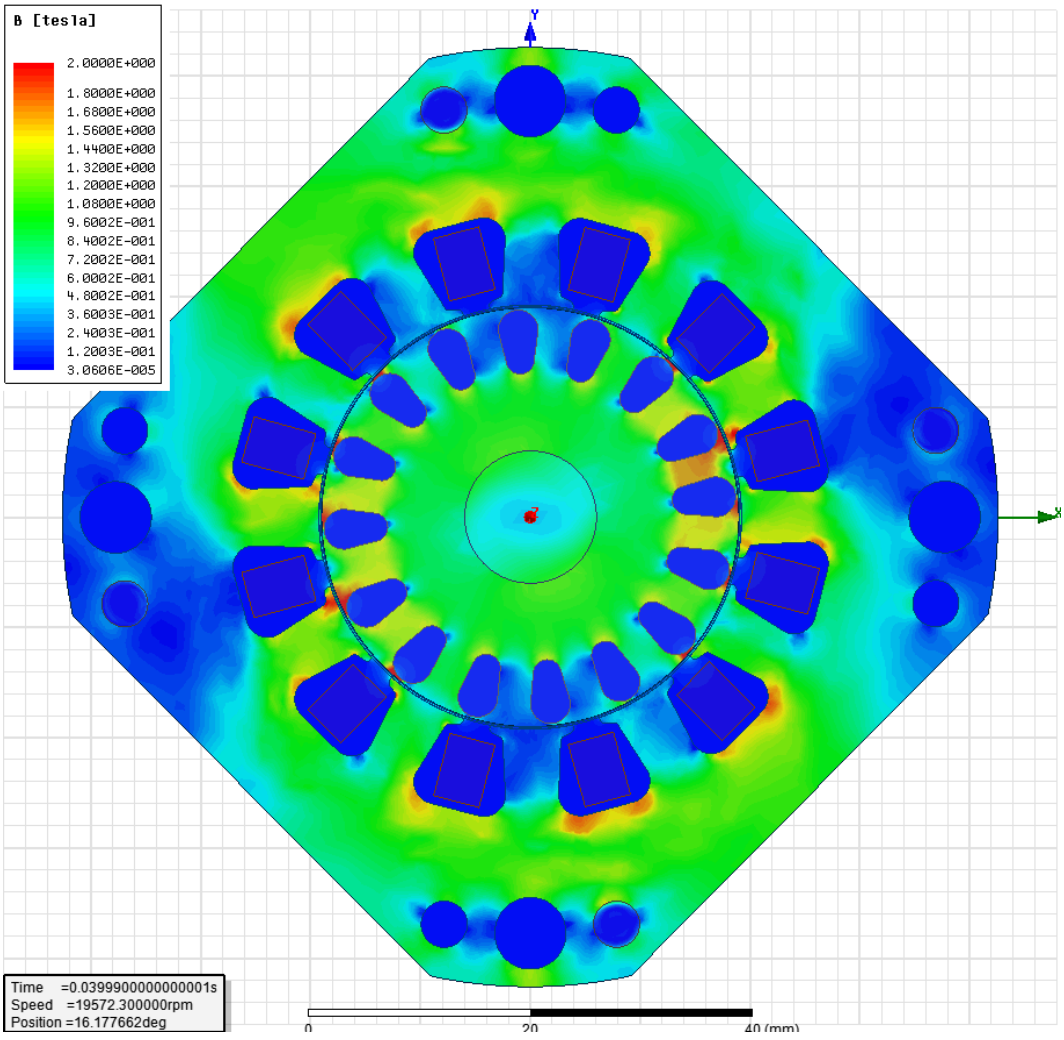

Figure 1: Distribution of magnetic flux density in test motor with all four rivets

3. PARAMETERS OF RIVETS

Test motor was after no-load test disassembled and resistivity between rivets and rivets itself were measured. Isolations in rivets ending were ruined and several measurements of resistance R_n = 24.42 μΩ between each rivets was taken. Then all four rivets, who hold stator stack together, were removed. To obtain electrical resistance R_r of one rivet, one piece of rivet was measured several times and average value was recalculated to the length of stator stack. Relative resistance ρ_r can be calculated where resistance R_r, area S_r and length of stator stack l_{Fe} are known. Relative conductivity σ_r of one rivet is then inverted value.

$$\rho_r = \frac{R_r \cdot S_r}{l_{Fe}} = \frac{0.486 \cdot 10^{-3} \cdot 12.56 \cdot 10^{-6}}{50 \cdot 10^{-3}} = 1.206 \cdot 10^{-7}\ \Omega \cdot \mathrm{m} \qquad (1)$$

$$\sigma_r = \frac{1}{\rho} = \frac{1}{1.206 \cdot 10^{-7}} = 829352442\ \mathrm{S/m} \qquad (2)$$

It can be assume, that all four resistance R_r of rivets are the same. The true value of resistance between rivets R_x is needed to be calculated. Measurement between two rivets did take into account the other parallel path as it can be seen from Fig. 2. To obtain electric resistivity between two rivets, the electric circuit in Fig.2 has been solved. The value of resistance R_X = 64.5 mΩ in circuit in Fig.2 was changed until the resistance calculated from V-meter and A-meter shown a measured value R_n = 24.42 μΩ from measurement.

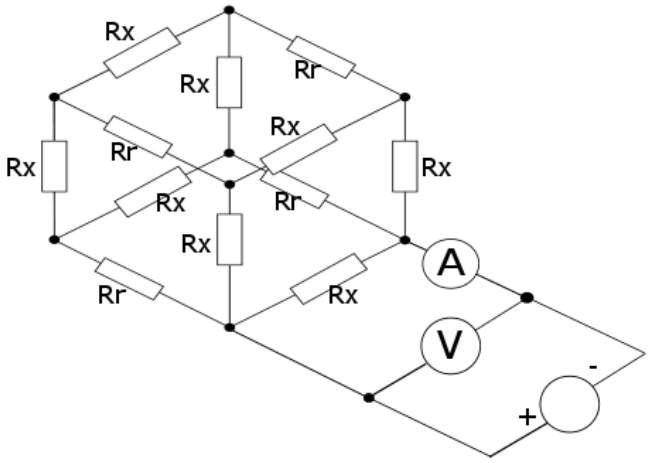

Figure 2: Electric circuit of four rivets

4. TEST BENCH

Test bench was used, as it can be seen in Fig.3, to experimentally verify data from simulation. Our laboratory space was equipped with proper devices. Motor was fed from laboratory power supply AMETEK 5001iX with very low harmonic distortion. The input power, voltages, currents and power factor were measured by YOKOGAWA WT 1800. Torque and velocity was measured by torque sensor TORQUEMASTER. The stator sheets are riveted. It can be seen from Fig. 1 that stator sheets have several drills for rivets. The influence of the riveting is subject of interest. Motor was measured under no-load condition with and without rivets.

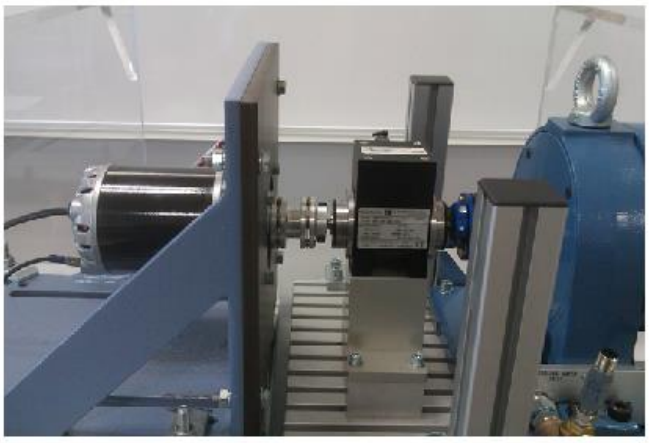

Figure 3: Motor coupled with dynamometer

To obtain mechanical and core loss of the motor, the no–load test was used. Motor was supplied from special laboratory source with very low total harmonic distortion. Supply frequency is f=330 Hz. Data obtain from no–load measurement is in table 1 and 2. P_c represent core losses, P_0 is input power, P_m mechanical loss by ventilation and friction, P_j is joule loss in stator winding, U_0 is input phase voltage and I_0 is input current.

U_0	I_0	P_j	P_m	P_0	P_c
[V]	[A]	[W]	[W]	[W]	[W]
95.04	3.18	15.69	97.05	225.00	110.5

Table 1: Data obtain from no-load measurement with rivets

U_0	I_0	P_j	P_m	P_0	P_c
[V]	[A]	[W]	[W]	[W]	[W]
95.03	3.218	15.06	102.38	231.8	112.36

Table 2: Data from no-load measurement without rivets

Test motor was measured under load condition too. There were several measurement with variable output torque M_z. One point from measuring, with output torque M_z = 0.39 Nm, was taken and it served to compare measured data with simulation. The results can be seen in table. 3. Losses were distributed in accordance to ČSN EN 60034-2.

5. RESULTS

Quantity	Measurement	Simulation of FE model		Unit
		Rivets	No-rivets	
Mechanical speed	19572.3	19572.3	19572.3	[rpm]
Line voltages	180 (*) 165 (**)	165	165	[V]
Stator current	5.453	4.948	4.941	[A]
Input power	1164.5	1116.96	1116.47	[W]
Winding loss	46.18	37.9	37.9	[W]
Rotor loss and rivets	11.29	22.3	22	[W]
Core loss	107.73	105.31	105.24	[W]
Mechanical loss	97.05	97.05	97.05	[W]
Total loss	365.3	280.21	280.23	[W]
Output power	799.2	836.75	836.24	[W]
Output torque	0.39	0.408	0.408	[Nm]
Residual losses	103.05	17.65	18.04	[W]

*) the rms value of the supply voltage spectrum
**) the rms value of the first harmonic of supply voltage

Table 3: Comparison of measurement with fem model with and without rivets

Power loss of one rivet P_{rivet} with length related to stator stack has been calculated in field calculator in ANSYS Maxwell from expression (3) and (4):

$$p_{rivet}(t=44\,\text{ms}) = l_{\text{Fe}} \cdot \int \overline{E} \cdot \overline{J}\, dV = l_{\text{Fe}} \cdot \int \frac{\overline{J} \cdot \overline{J}}{\sigma_{\text{r}}} dV = 0.0483\,\text{W} \tag{3}$$

$$P_{rivet} = \frac{1}{T} \cdot \int_{t}^{t+T} p_{rivet}(t) \cdot dt = 0.0309\,\text{W} \tag{4}$$

Where $\overline{J}$ is current density, $\overline{E}$ is electric field strength, l_{Fe} is length of stator stack, ρ_{r} is electric conductivity of one rivet and T is time of one period.

6. CONCLUSION

This paper deals with analysis of high speed squirrel cage induction motor. Test motor was tested on bench to experimentally verify the results. In first comparison, motor was supplied from laboratory source. The major divergence between calculated and measured results are because of input power. It can be seen, from table II, that measured input power is higher than input power from simulation. The difference can be composed of several aspects. One aspect can be made by inaccuracy of measurement.

Motor is supplied by frequency of f_s=330 Hz and thus even a small difference between the real value of torque and measured one can make a different value of the output power. Another portion of

loss are made by friction in coupler between motor and dynamometer and finally the input voltage in measurement contain higher harmonics. The difference in rms value between voltage spectrum and voltage first harmonic is 15V.

In second comparison, the simulations with and without rivets were performed. Mechanical loss was taken from no-load measurement and it was steady value for all three simulations. Output torque was obtained as a difference between calculated inner torque by Maxwell and torque of mechanical loss. It can be seen from table 3. that distribution of losses are almost identical. The losses in rivets are computed by solid loss computation in ANSYS Maxwell where Maxwell integrate current density square over the volume of rivets. The difference between riveting and not-riveting state is minimal and therefore field calculator was used to confirm and refine the results. Results have shown that power losses in rivets are very small and have minimal influence.

No-load measurement described in chapter 4. was performed and it can be seen from the results that differences were especially in mechanical losses and core losses. Mechanical losses increase after first no-load test with rivets because of disassembling and assembling of the motor. Core loss in non-riveting state is slightly higher than with rivets. Rivets were not removed according the plan. Rivets were drilled out and therefore exist the possibility that isolation between sheets can be ruined. Difference between measured and simulated core loss (see table 3) is mainly because of manufacturing process.

ACKNOWLEDGMENT

This research work has been carried out in the Centre for Research and Utilization of Renewable Energy (CVVOZE). Authors gratefully acknowledge financial support from the Ministry of Education, Youth and Sports of the Czech Republic under NPU I programme (project No. LO1210)

REFERENCE

[1] H. Zhou and F-X. Wang, “Comparative study on high speed induction machine with different rotor structures,” in Proc. Int. Conf. Elect. Machines Syst., Seoul, Korea, Oct. 8–11, 2007, pp. 1009–1012

[2] J. HUPPUNEN, *High-speed solid-rotor induction machine: electromagnetic calculation and design*. Lappeenranta: Lappeenrannan Teknillinen Yliopisto, 2004. ISBN 95-176-4981-9.

[3] Lähteenmäki Jussi, *Design and Voltage Supply of High-Speed Induction Machines*, Dissertation for the degree of Doctor of Science, Helsinky University of Technology, Finnish Academies of Technology 2002

[4] Hilinski, E.J.; Johnston, G.H., "Annealing of electrical steel," *Electric Drives Production Conference (EDPC), 2014 4th International* , vol., no., pp.1,7, Sept. 30 2014-Oct. 1 2014

[5] TONG, Wei. *Mechanical Design of Electric Motors*. CRC Press, 2015. ISBN 9781420091441.

[6] Krings, A.; Nategh, S.; Wallmark, O.; Soulard, J., "Influence of the welding process on the magnetic properties of a slot-less permanent magnet synchronous machine stator core,"*Electrical Machines (ICEM), 2012 XXth International Conference on* , vol., no., pp.1333,1338, 2-5 Sept. 2012

[7] PATOČKA, Miroslav. *Magnetické jevy a obvody ve výkonové elektronice, měřicí technice a silnoproudé elektrotechnice*. 1. vyd. V Brně: VUTIUM, 2011, 564 s. ISBN 978-80-214-4003-6.

[8] Maxwell 2D Online Help; ANSYS Inc, 628p.